
Similarity as Reward Alignment: Robust and Versatile Preference-based Reinforcement Learning

Sara Rajaram¹⁻³ R. James Cotton⁴ Fabian H. Sinz¹

¹ Institute for Computer Science and Campus Institute for Data Science,
University of Göttingen, Göttingen, Germany

² University Hospital Tübingen, Tübingen, Germany

³ International Max Planck Research School for Intelligent Systems, Tübingen, Germany

⁴ Shirley Ryan Ability Lab, Northwestern University, Chicago, USA

Abstract

Preference-based Reinforcement Learning (PbRL) entails a variety of approaches for aligning models with human intent to alleviate the burden of reward engineering. However, most previous PbRL work has not investigated the robustness to labeler errors, inevitable with labelers who are non-experts or operate under time constraints. Additionally, PbRL algorithms often target very specific settings (e.g. pairwise ranked preferences or purely offline learning). We introduce Similarity as Reward Alignment (SARA), a simple contrastive framework that is both resilient to noisy labels and adaptable to diverse feedback formats and training paradigms. SARA learns a latent representation of preferred samples and computes rewards as similarities to the learned latent. We demonstrate strong performance compared to baselines on continuous control offline RL benchmarks. We further demonstrate SARA’s versatility in applications such as trajectory filtering for downstream tasks, cross-task preference transfer, and reward shaping in online learning. Our code is publicly released.¹

1 Introduction

Reinforcement Learning (RL) algorithms rely on carefully engineered reward functions in order to produce the desired behaviors for a task of interest [1, 2]. In complex real-world settings, reward engineering requires various sensors, such as motion trackers [3] or computer vision systems [4], as well as tedious hand-crafting to fine-tune such functions [5] and ensure safe behavior [6]. To mitigate reward engineering challenges, Preference-based RL (PbRL) algorithms have garnered increased attention in recent years. In a PbRL setting, human labelers provide feedback on a dataset of agent behaviors, and the PbRL algorithms aim to learn agent models that produce behavior better aligned to the preferences. Prominent examples include Large Language Model (LLM) fine-tuning [7–10] as well as robotics and simulated control [11, 12].

PbRL methods can learn a reward function from human feedback to use in downstream RL, but they face the challenge of accurately representing preferences from limited data [13]. Many prior works leverage preference labels on trajectory pairs by applying the Bradley-Terry (BT) model [14]:

$$P[\sigma^1 \succ \sigma^0; \psi] = \frac{\exp(\sum_t \hat{r}(s_t^1, a_t^1; \psi))}{\exp(\sum_t \hat{r}(s_t^1, a_t^1; \psi)) + \exp(\sum_t \hat{r}(s_t^0, a_t^0; \psi))}$$

¹<https://github.com/sinzlab/sara-pbri>

where σ^1 and σ^0 are sampled preferred and non-preferred trajectories, respectively, and \hat{r}_ψ is a learnable reward function. The BT model is often used to learn an explicit reward function \hat{r}_ψ [12, 15, 16, 9, 6] or re-formulated to learn a policy without a reward model [17–22].

In both cases, the BT model formulations come with assumptions and limitations, discussed by previous works [23–27]. The BT model assumes that human preferences are transitive, an assumption which has been undermined by psychology research [27–29]. Azar et al. [26] showed that the BT reward models can overfit to the relative rankings in the trajectory pairs, resulting in agent behavior that also overfits to the preferred ranked trajectory. Overfitting is particularly problematic when labels are noisy or behaviors are similar. Labeling errors occur when annotators are time-constrained or non-experts [27, 30]. Realistic error rates are between 5-38% [23], as evidenced by an observed 25% disagreement rate among labelers [31, 32]. Prior work demonstrated that even a 10% label error rate can significantly degrade RL performance [33, 30]. Sun et al. [23] show that the BT-model is not a necessary choice for a reward modeling approach, and BT-based models result in underperforming behaviors when labeling error rates are above 10%.

In contrast to most works, we assume the presence of labeling mistakes and similar behaviors in ranked pairs, so we avoid learning BT-modeled rewards based on the relative labels. To this end, we introduce Similarity as Reward Alignment (SARA), a robust and flexible PbRL framework. SARA acknowledges that even with noise, discerning patterns exist in the preferred set as a whole and employs contrastive learning to obtain a representation for this set. SARA then computes rewards at each timestep based on the encoded trajectory’s similarity to the preferred representation. Despite its simplicity, this formulation handles noisy or ambiguous preference data reliably, and to our knowledge, our framework is novel in the PbRL literature. Our contributions and findings are:

Strong performance and robustness. Compared to state-of-the-art baselines, SARA achieves competitive or superior performance using script-labeled and human-labeled preference datasets. We also vary the preference data by injecting label noise and examining effects of including vs excluding equally ranked preferences. In preference sets on control tasks with 20% label error rate, SARA achieves a 31% average improvement in policy evaluation rewards over baselines. Moreover, SARA’s policy evaluation rewards are relatively stable to variations in the preference data. By contrast, baselines fluctuate up to 73% comparing without and with noise.

Versatile preference modeling. The performance of a particular RL algorithm can depend greatly on task complexity and in the offline case, the amount of low return trajectories [34, 35, 19]. This is evident when comparing performance of popular offline algorithms ([36], Table 1). The methods that do not learn an explicit reward network, as in [20, 17, 19, 22], typically can not provide reward values for sampled trajectories. Therefore, they cannot be easily integrated into any off-the-shelf offline or online RL algorithm. They also cannot add preference rewards to task rewards in cases where they are known. SARA enables flexibility by allowing for reward inference, and it also can accept different feedback types, rather than requiring pairs.

Additional applications.

Low-Reward Trajectory Detection: The SARA contrastive encoder can identify low-reward trajectories, even if they are labeled as preferred. This feature allows for a trajectory filtering method for downstream Imitation Learning.

Cross-Task Preference Transfer: SARA enables transferring preferences on movements of an agent with a simple morphology to estimate rewards for a more complex agent’s movements (e.g. one-legged hopper to two-legged walker).

Reward Shaping in Online RL: SARA can complement known task rewards with preference-inferred rewards, useful in settings like robotics where task rewards may not fully capture desired style behavior. We demonstrate this with a cherry-picked preference set rather than ranked pairs. We simply add inferred rewards to environment provided rewards in an online RL algorithm. This highlights SARA’s adaptability to reward shaping in online RL and to different feedback types.

In summary, SARA is broadly applicable across diverse settings, including online and offline RL, expert and non-expert labelers, presence or absence of neutral preferences, human or scripted labels, trajectory pairs or sets of preferred trajectories, and the aforementioned interesting problem setups.

2 Related work

Preference-based RL Enabling development and comparison of PbRL algorithms, Kim et al. [6] provided both expert-human labeled and script-labeled preference datasets for D4RL offline benchmark tasks. They also proposed the Preference Transformer (PT) reward model trained with a BT-based loss function to learn from preference data. As reward models can fail to capture true underlying preferences with limited data, subsequent works developed methods that avoid learning a reward model [18, 17, 19, 20, 22, 37, 38]. Inverse Preference Learning [18] reformulates the BT model in terms of the RL Q-function, and can be used both in online and offline learning. In a similar vein of avoiding reward modeling, Offline Preference-guided Policy Optimization (OPPO) learns a trajectory encoder, an optimal latent, and learns a Decision Transformer policy conditioned on the latents [20].

Contrastive learning in PbRL Contrastive Preference Learning (CPL) generalizes the BT model and uses contrastive learning on the discounted sum of log policy for preferred and non-preferred segments [17]. CPL reformulates policy learning as a supervised learning objective rather than RL. Direct Preference-based Policy Optimization (DPPO) learns a BT-based preference predictor network, infers preferences for a full offline dataset, and lastly conducts contrastive learning to align policy predictions with the inferred preferred trajectories [19]. Learning to Discern (L2D) conducts contrastive learning between trajectories of different labels [22]. They then train a network with a BT-based loss, and its output is mapped to labels to filter low quality trajectories for downstream Imitation learning (IL).

Robustness in PbRL Though robustness techniques have been studied extensively in supervised learning contexts [39–43], relatively little attention has been given in PbRL to the effect of labeling noise. Cheng et al. [30] developed a PbRL method to filter out noisy preferences by defining a time dependent threshold for KL-divergence between predicted preference and the provided label. However, this framework involves querying human preferences iteratively online during policy training; it is not straightforward to adapt to our setting, in which the preference set is fixed and new queries cannot be sampled. Sun et al. [23] examine preference learning in an LLM context, and they showed theoretically that BT formulations are not necessary. Instead of a BT loss that predicts the probability of preferring one response over another, they propose a simple classifier approach of predicting binary response preference. Compared against BT based approaches, they showed improved performance on LLM human value metrics for label error rates above 10%.

Our work diverges from these previous works as follows. As discussed in Section 1, the vast majority of PbRL works rely on BT assumptions. Our work prioritizes representation learning and avoids BT-modeling due to the potential to overfit [26], especially problematic with noisy comparison labels [23]. Unlike the methods that do not learn an explicit reward function [20, 17, 19, 22], we use our representations to provide rewards which enables versatility to off-the-shelf offline and online RL algorithms (advantageous as discussed in Section 1). Also, if the problem setup has a known task reward, as occurring in a robotics setting, our method allows easy reward shaping by adding task rewards to preference inferred rewards. The classifier approach proposed by Sun et al. [23] lays out a theoretical foundation for a non-BT approach. However, they focus on the LLM bandit setting whereas we focus on RL environments, with multi-step state/action trajectories. Whereas they focus on label classification, we focus on representation learning and infer rewards cheaply afterwards.

3 Similarity as Reward Alignment (SARA)

We first review the PbRL setup. We then describe the SARA model, comprising a contrastive transformer encoder to learn a preferred set representation and a reward inference method. Appendix D provides details and hyperparameters.

Preliminaries In the RL paradigm, an agent at timestep t and state \mathbf{s}_t interacts with the environment by choosing an action \mathbf{a}_t . The action is chosen via its policy $\mathbf{a}_t = \pi(\mathbf{s}_t)$ which is a mapping from state to action. The environment provides reward $r(\mathbf{s}_t, \mathbf{a}_t)$ and transitions the agent to the next state \mathbf{s}_{t+1} . RL algorithms aim to learn a policy that maximizes the discounted cumulative reward, $R_t = \sum_{k=0}^{\infty} \gamma^k r(\mathbf{s}_{t+k}, \mathbf{a}_{t+k})$ with discount factor γ .

To address the reward engineering problem [1, 2], PbRL leverages human labeled preferences to learn policies that align with human intent [13]. Several previous approaches [12, 6, 18, 17, 19, 20] assume that human feedback is given in the form of preferences over trajectory pairs. Each trajectory segment

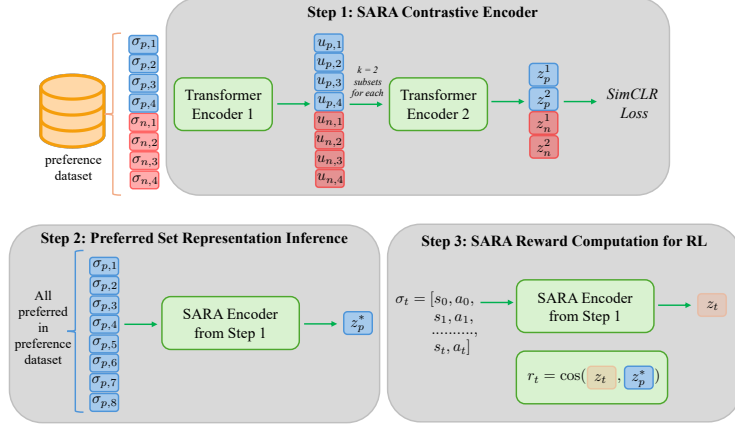


Figure 1: Step 1: preferred and non-preferred trajectories are extracted from labeled pairs. The first Transformer encodes each trajectory with the positional encodings of timesteps. We then divide each set $\{\mathbf{u}_{p,i}\}$ and $\{\mathbf{u}_{n,i}\}$ into k subsets; the composition of encodings in each subset is shuffled each iteration. The second Transformer encodes each subset. The SimCLR loss aligns latents \mathbf{z} of same category. Step 2: infer \mathbf{z}_p^* from full preference set. Step 3: compute reward for a sampled trajectory in offline or online RL training

σ consists of H state-action transitions: $\sigma = \{(s_0, a_0), (s_1, a_1), \dots, (s_{H-1}, a_{H-1})\}$. Given a pair of segments (σ^0, σ^1) , a human annotator provides a preference label $y \in \{0, 0.5, 1\}$. The labels $y = 0$ and $y = 1$ indicate $\sigma^0 \succ \sigma^1$ and $\sigma^1 \succ \sigma^0$, respectively. The neutral preference $y = 0.5$ designates equal preference between the two trajectories.

SARA contrastive encoder Assume we are given a set of preferred trajectories and a set of non-preferred trajectories. In contrast to the common setting described above, we do not assume that the trajectories are given in pairs. As a consequence, the sets can also have different sizes. In our experiments on data where labeled pairs are provided, we break apart the pairs to form the two sets, so we do not preserve the provided ranking between the two trajectories. If pairs with neutral preference ($y = 0.5$) are in the dataset, we place both trajectories in both sets.

We design our contrastive encoder to yield latent representations for sets of trajectories. To that end, all trajectories are passed through Transformer Encoder 1 with positional encodings of timesteps [Figure 1, 44], followed by average pooling over timesteps to obtain a single encoding per trajectory. This yields trajectory encodings $\mathbf{u}_{p/n,i}$, where p or n indicates preferred or non-preferred and i indexes the trajectory. Next we form k subsets within each category, *i.e.* k subsets within the set of $\{\mathbf{u}_{p,i}\}$ and k subsets within the set of $\{\mathbf{u}_{n,i}\}$. Then we pass each subset $\{\mathbf{u}_p\}_k$ and $\{\mathbf{u}_n\}_k$ through Transformer Encoder 2, enabling encodings in the same subset to attend to each other. Subsequently, we obtain a single encoding $\mathbf{z}_{p/n,k}$ for each subset. We train the encoder using the SimCLR contrastive loss [45] to push together the preferred subset latents $\mathbf{z}_{p,k}$ and separate them from non-preferred latents $\mathbf{z}_{n,k}$.

During training, we randomize the composition of trajectory encodings in each subset $\{\mathbf{u}_p\}_k$ and $\{\mathbf{u}_n\}_k$ with each epoch of training. Doing so encourages robustness because the encoder is forced to align and differentiate between varying compositions. The encoder must learn patterns of behavior which distinguish the two categories even when some trajectories are quite similar. If some trajectories are mis-labeled or if some are the same (due to presence of neutral queries), the transformer can learn to ignore these similarities when distinguishing preferred from non-preferred. The additional benefit of the transformer architecture is that we can encode sets of inputs, and the number of trajectories within a set can vary. Thus we can train on subsets $\{\mathbf{u}_p\}_k$ of any size during training, but at inference we can feed in the full set of preferred trajectories into the learned encoder. Doing so gives us \mathbf{z}_p^* , a fixed representation of preferences (Figure 1, Step 2). We use this frozen preferred latent \mathbf{z}_p^* to get our similarity reward.

SARA reward inference For each trajectory up to time t , we get the latent $\mathbf{z}_t = \mathcal{E}(\sigma_t)$, where \mathcal{E} is the trained and frozen encoder. Then we simply compute the reward at time t as: $r_t = \cos(\mathbf{z}_t, \mathbf{z}_p^*)$

using our frozen preferred latent (Figure 1, Step 3). This is a simple yet novel proposal for reward estimation from preferences. Appendix A provides theoretical motivation for this reward formulation.

4 Offline RL experiments

In this section we address the following questions: First, how does using SARA inferred rewards compare to prior PbRL algorithms in the domain of offline RL? Secondly, how does SARA perform when the dataset is modified, *i.e.* neutral preferences are excluded or labeling mistakes occur?

Setup Similar to past works [6, 19], we evaluate our framework in the offline setting on the following D4RL benchmark datasets: Mujoco locomotion (4 datasets), Franka Kitchen (2 datasets), Adroit (2 datasets) [46–48]. For the Mujoco and Adroit tasks, we use the preference datasets provided by Kim et al. [6]. We use the datasets by An et al. [19] for the Kitchen tasks. All preference datasets comprise a limited subset of labeled trajectory pairs (100-500 pairs, depending on the dataset) relative to the full number of offline trajectories. The Adroit and Kitchen tasks have high dimensional state/action spaces (69 state+action dimensions) relative to the Mujoco tasks (14-23 state+action dimensions). Thus, our experiments comprise a variety of task environments, labeler sources, and state-action dimensionalities. Additional details on the preference and full offline datasets can be found in Appendix C.1. The policy evaluation rewards exhibit high variance and are quite similar across models for the Adroit tasks, so we defer the Adroit results to Appendix B.2.

After training on preference datasets, we compute the rewards r_t , as discussed in Section 3, for all transitions in the full offline dataset. We conduct offline RL training with the state-of-the-art Implicit Q-Learning (IQL) algorithm [36], as in several prior PbRL works [6, 36]. We adapt the OfflineRL-kit IQL implementation for our purposes [49], and we match preprocessing steps and hyperparameters to the recommended values in [36, 6] (Appendix D). We train SARA+IQL, oracle IQL, and baselines on 8 seeds with multiple evaluation episodes (see Appendix E.2 for reward normalization method and reward reporting method). IQL trained on oracle datasets, with true environmental rewards, are included in each table for easy reference, but they are the same in all tables.

We compare against the following baselines. The first two baselines (PT, PT+ADT) learn a reward model from the preference dataset and then conduct IQL training. The last baseline does not learn an explicit reward model (DPPO).

- **Preference Transformer (PT):** As in our model, PT uses a transformer backbone [6]. Unlike our model, PT learns an explicit reward model with a BT based loss.
- **PT with Adaptive Denoising Training (PT+ADT):** We introduce this novel application of ADT as a baseline. In each training step, ADT drops a $\tau(t)$ fraction of queries with the largest cross-entropy loss, where $\tau(t) = \min(\gamma t, \tau_{\max})$ [39]. We set $\tau_{\max} = 0.3$ and $\gamma = 0.003$ for our datasets. Prior works have considered ADT in the setting of iterative online human feedback [30], but to our knowledge we are the first to apply ADT to learning the PT reward model.
- **Direct Preference-based Policy Optimization (DPPO):** As in our model, DPPO relies on contrastive learning and does not learn an explicit reward model. However, the contrastive learning is used to learn the policy directly and aims to align policy predictions with inferred preferred trajectories [19] (see Section 2 for additional details).

Preference data with labeling noise We take the original preference datasets and randomly flip 20% of the non-neutral labels. As shown in Table 1, the IQL policy with SARA computed rewards substantially outperforms baselines. Even with labeling errors, it performs comparably to the Oracle IQL (which uses true environmental rewards) for all datasets except for the hopper replay. In addition, even on this dataset, it achieves much lower variance compared with the oracle. Finally, our novel implementation of PT+ADT also provides significant improvement over PT.

Performance with original preference datasets Here we show model performances with the original unmodified preference sets. With the exception of the hopper-expert dataset, SARA either outperforms or is on-par with baseline methods. On expert datasets (hopper and walker 2d) without noise, DPPO achieves strong performance. We infer that DPPO is able to match expert trajectories in such datasets with many examples. However, flipping labels substantially degrades DPPO’s performance on hopper-expert (Table 1).

Table 1: Average normalized policy evaluation rewards (across 8 seeds), using **human-labeled preference data with 20% mistakes**. Values in **bold** are best (highest reward) in each row and underlined are within 1% of best. The \pm denotes standard deviation.

Task	IQL (Oracle)	PT	PT+ADT	DPPO	SARA
hopper-replay	92.26 \pm 13.6	49.77 \pm 25.7	62.87 \pm 24.0	68.67 \pm 19.8	82.94 \pm 5.8
hopper-expert	80.82 \pm 44.5	68.14 \pm 36.2	79.02 \pm 21.0	28.92 \pm 29.1	85.16 \pm 17.0
walker2d-replay	77.53 \pm 15.5	71.73 \pm 10.7	74.42 \pm 12.6	41.00 \pm 26.8	76.29 \pm 13.2
walker2d-expert	107.57 \pm 8.5	<u>109.37</u> \pm 1.5	109.53 \pm 1.6	<u>108.78</u> \pm 0.4	108.37 \pm 5.7
kitchen-partial	44.88 \pm 31.4	58.55 \pm 18.6	60.55 \pm 16.7	38.44 \pm 19.3	64.18 \pm 15.4
kitchen-mixed	54.02 \pm 16.4	44.65 \pm 16.9	41.60 \pm 20.5	46.05 \pm 18.4	49.02 \pm 13.5

Table 2: Average normalized policy evaluation rewards (across 8 seeds), using **human-labeled preference data with neutral preferences**. Values in **bold** are best (highest reward) in each row and underlined are within 1% of best. The \pm denotes standard deviation.

Task	IQL (Oracle)	PT	PT+ADT	DPPO	SARA
hopper-replay	92.26 \pm 13.6	74.48 \pm 21.3	80.24 \pm 16.1	68.98 \pm 18.4	84.68 \pm 3.1
hopper-expert	80.82 \pm 44.5	89.64 \pm 28.3	71.33 \pm 40.6	108.09 \pm 10.8	80.45 \pm 48.1
walker2d-replay	77.53 \pm 15.5	74.43 \pm 8.0	75.68 \pm 8.3	47.21 \pm 28.0	78.21 \pm 5.8
walker2d-expert	107.57 \pm 8.5	<u>109.74</u> \pm 1.1	109.98 \pm 1.0	108.73 \pm 0.4	108.35 \pm 5.4
kitchen-partial	44.88 \pm 31.4	<u>59.45</u> \pm 15.6	61.68 \pm 15.2	40.39 \pm 18.9	64.84 \pm 13.2
kitchen-mixed	54.02 \pm 16.4	<u>53.32</u> \pm 9.8	53.48 \pm 9.7	43.63 \pm 17.9	50.51 \pm 6.4

Robustness to dataset variants Here we explore the consistency of our model to additional dataset variants, such as exclusion of neutral preferences and script labeling. In many realistic applications, labelers are often presented with queries where the two options are quite similar. In some designs, for example current OpenAI GPT models, the labeler is forced to pick a preferred option. In others, as in the dataset by Kim et al. [6], the labelers are allowed to indicate indifference (Appendix C.1 provides percentage of neutral queries per dataset). The performance of the learned policy should ideally not have strong sensitivity to such choices. A PbRL framework exhibits robustness by its ability to discern patterns of preferences, and those learned patterns should not be contingent on whether or not neutrality is allowed. Script labeling, in which an oracle with knowledge of task rewards picks binary preferences based on comparisons of total returns, has also been examined in prior works [6, 38, 20, 12, 30]. As human labelers are known to disagree at rates up to 25% [31, 32], performance on script labeling provides another method of comparing models. Figure 2 shows the four models on the four dataset variants. We exclude the walker expert dataset as it is high performing and consistent across models. Comparing the vertical range of values spanned by each model for a given dataset, we see that SARA is quite consistent across dataset variants as well as performant. By contrast, PT and DPPO exhibit dramatic fluctuations on the hopper datasets, with up to 73% changes in rewards. Our novel baseline PT+ADT is also consistent but tends to underperform compared to SARA. See Appendix B.1 for tables with exact values and error bars.

Offline experiments summary In preference sets with 20% label error rate, SARA achieves a 31% mean relative gain in policy evaluation rewards over baselines. SARA displays very consistent performance across the four preference dataset variants, whereas baseline models show large fluctuations or underperform relative to SARA (Figure 2).

5 Additional experimental applications

Here we provide additional applications our framework naturally supports. The experiments detailed in this section suggest novel avenues to further explore in future works.

Filtering low quality trajectories for downstream imitation learning As ground truth rewards may be unknown, we examine whether the SARA encoder can identify low quality trajectories from preference data. Human preference labels and ground truth rewards frequently do not align [6], so

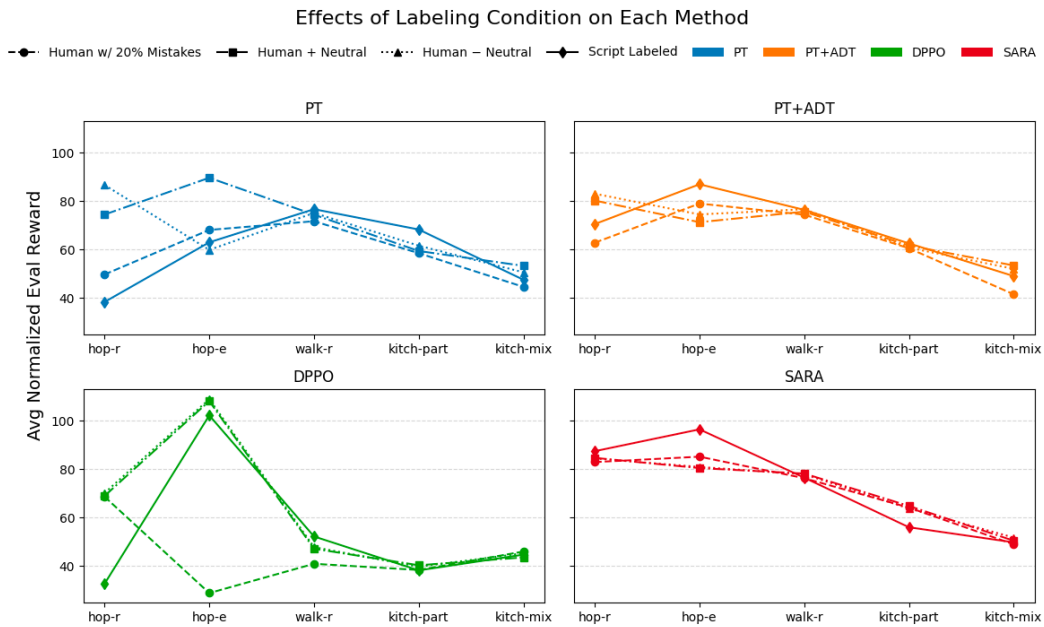


Figure 2: Average normalized policy evaluation rewards are shown for four preference set variants across five tasks (hop-r denotes hopper-replay and so on). The plot shows the impact of preference set variation on each model’s performance. Standard deviations are provided in Tables 1, 2, 3,4.

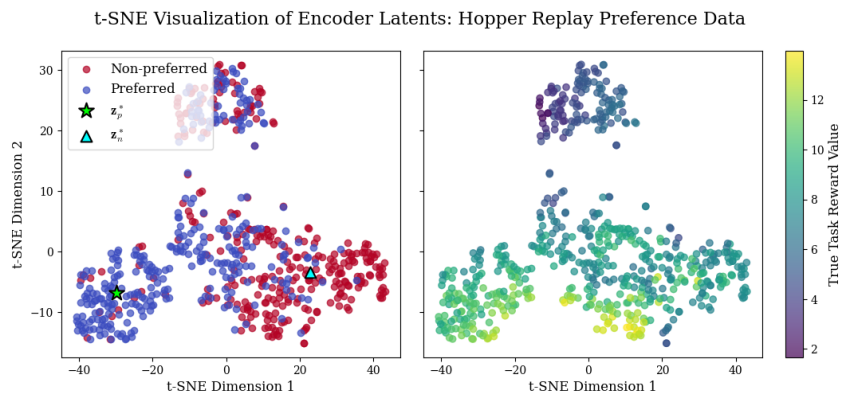


Figure 3: T-SNE embedding of the latents for the hopper-medium-replay-v2 preference data, either colored by preference (left) or true reward (right).

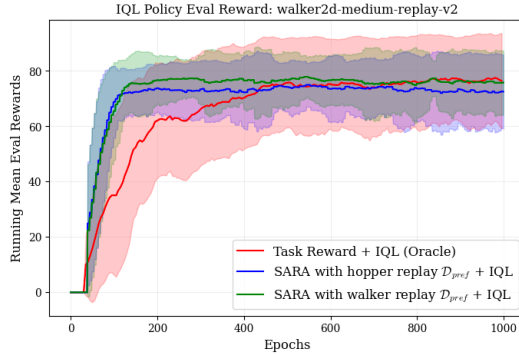


Figure 4: Walker2d IQL eval rewards, running average and 8 seeds (see Section E.2). Shading indicates standard deviation. The policy is learned on the walker replay dataset. SARA rewards from training on hopper replay preferences perform almost as well as SARA rewards with training on the walker replay preferences.

many poor quality trajectories may be labeled preferred ($y = 1$). Figure 3 shows a t-SNE plot of SARA learned latents for the human labeled hopper replay preference dataset from Kim et al. [6]. We exclude the neutral queries from the original preference dataset, but we otherwise do not corrupt or modify the dataset in any way. As encouraged by the contrastive learning objective, the encoder achieves good separation and clustering between *most* preferred and non-preferred trajectories, and the group embeddings \mathbf{z}_p^* and \mathbf{z}_n^* are centrally located within their respective clusters. However, some trajectories are not close to \mathbf{z}_p^* nor \mathbf{z}_n^* , though they are labeled as such. Comparing the plots in Figure 3, we see that these separated trajectories exhibit a low ground truth reward. Therefore, the SARA encoder can learn overall patterns but it does not artificially align poor quality trajectories to the preferred set even when the human labelers designate them as preferred. This result is an explanation for the observed robustness evidenced in previous sections. We can further exploit the encoder results to filter low quality trajectories. After training the encoder, we merely need to filter out trajectories with large distance in latent space from both \mathbf{z}_p^* and \mathbf{z}_n^* . Kuhar et al. [22] notes that filtering should lead to a better policy in downstream IL. As IL is outside the scope of this work, we defer such analysis to future works.

Transfer of preferences to morphologically harder task We investigate whether the preference dataset for a morphologically simple task can be used to infer rewards for a harder task. We take the preference dataset from Kim et al. [6] for trajectories from hopper-medium-replay-v2. Our goal is to learn the SARA encoder on this preference set and then infer rewards for the walker-medium-replay-v2 dataset. SARA reward inference relies on feeding walker trajectories into the learned encoder, so we map the state and action space dimensions of the hopper to that of the walker. We do so by crudely assuming that preferences for the hopper state-action trajectories can transfer to the additional degrees of freedom in the walker due to the symmetry of the joints (see Appendix F for details).

After doubling the joint angles, velocities, and torques in the hopper replay preference set, we then train the SARA encoder with this modified set. Next we take the full offline walker replay set and infer rewards using this encoder learned from the hopper preferences. This cross-task transfer of preferences enables policy learning with these estimated rewards (Figure 4). Remarkably, the IQL learned policy from cross-task preferences performs only slightly worse than the SARA model using the walker replay preference set. Both exhibit lower variance than using the true task reward.

Hejna et al. [50] investigated transfer learning of a policy from a simple agent to a more complex one with environment provided rewards, not preference aligned rewards. Liu et al. [51] proposed an optimal transport method to transfer preferences, but their framework is limited to tasks with equivalent state-action space. To our knowledge, our cross-task preference transfer to a larger state-action space is novel, and we do so without any changes to the SARA architecture or hyperparameters.

Online RL with reward shaping In contrast to previous sections, we now consider the scenario of some known but under-specified task reward. For instance, consider a robotics application in which a policy is trained to achieve some task, such as reaching an object. In many realistic applications, such

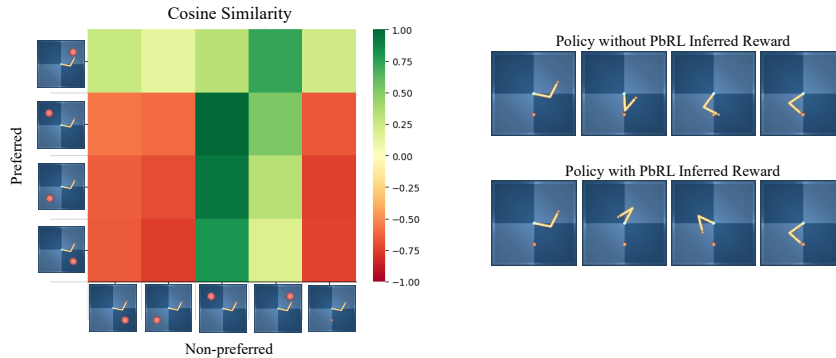


Figure 5: Left: After training SARA encoder, we divide up the trajectories by their label (preferred vs non-preferred) and by the target location. Note that the training set has the extra hard target location for the non-preferred but not preferred. Target location is not explicitly fed into the model and many trajectories are the same between the two sets. Right: With task reward alone, the learned policy takes the shortest path going clockwise to the hard target location. Including the preference inferred reward enables a learned policy traversing in counter-clockwise direction.

task-driven reward functions can result in policies that have undesirable patterns of movement, such as rapid or jerky actions [52]. Such movements may not only be visually unappealing but can also damage the robot. Prior works employed complicated reward shaping techniques to overcome these issues [53]. Here we test whether the SARA inferred rewards can shape the task reward in online RL learning.

We set up the following problem using the Deepmind Control Suite Reacher task [54, 55]. Let us assume a human labeler decided that counterclockwise movements are always preferable, perhaps due to a realistic engineering constraint or potential environmental obstructions limiting clockwise movement. The human labeler picks the preferred set of trajectories (all counterclockwise) for an easy target. The human labeler deems non-preferred any trajectories from the policy trained on the task reward. These are sometimes clockwise and sometimes counterclockwise depending on which has the fewest steps to target. Therefore, when the target is in the upper half, we have many trajectories for which the preferred and non-preferred sets overlap. This setup requires SARA to disentangle the preferred from non-preferred styles even when there are some strong similarities between the two groups.

The encoder is not explicitly given the counter-clockwise preference, so we evaluate what it implicitly learns by comparing with non-preferred movements. After training we split up trajectories by category (preferred vs non-preferred) and target location to view the similarity map shown in Figure 5. Despite overlaps between categories, SARA learns where preferred and non-preferred behaviors align or diverge. This result arises from the subset contrastive encoding and shuffling detailed in Section 3.

Next we test whether these learned patterns transfer to the harder task of the small target shown in Figure 5. We learn online using the Deep Deterministic Policy Gradient algorithm [56]. We add the known task reward to the SARA inferred reward. In the absence of our SARA inferred reward, the learned Reacher policy takes the most efficient path clockwise to the hard target (Figure 5). With our preference inferred reward, the policy takes the desired counterclockwise path even though it results in a lower task driven reward. The SARA framework achieves this even though the preferred set only includes the easy large target task.

This toy experiment illustrates our model’s potential for the realistic preference driven goal of shaping an RL policy to conform with human desires. Such stylistic rewards may be both application specific and difficult to engineer, so inferring from preference data is a promising path forward.

6 Conclusion

Summary We introduce Similarity as Reward Alignment (SARA), a novel algorithm that prioritizes robustness by estimating preference-based rewards via similarity with a contrastively learned latent.

Rather than relying on BT-based rewards as commonly done in the literature, SARA assumes presence of noisy labeling and learns a representation of preferences. On most offline RL datasets examined, SARA shows comparable or improved performance over state-of-the-art baselines. With a 20% label error rate, SARA acquires 31% mean improvement over baselines in mean policy returns. We demonstrate SARA’s versatility to under-explored application areas: filtering low quality trajectories, transfer of preferences to a morphologically harder task, and online RL with reward shaping. The latter case additionally demonstrates SARA’s adaptability to off-the-shelf online RL frameworks, and its utility when human feedback is not in relative paired form.

Limitations and future work Although we provide theory driven motivation for our framework in Appendix A, our work would benefit from a full theoretical treatment of the proposed cosine-similarity based reward function as it relates to preference modeling. Future application of the SARA framework to LLMs is an exciting prospect. We suggest adapting SARA for querying human preferences iteratively online during policy training. Doing so would require updating the encoder online as a human labeler provides feedback throughout policy training. Such setups are practically useful in LLM training where model updates are expensive. Lastly, our additional experiments (Section 5) warrant further exploration to different domains.

Acknowledgments and Disclosure of Funding

SR and FHS received funding through the Else Kröner Medical Scientist Kolleg “ClinbrAIn: Artificial Intelligence for Clinical Brain Research”. This work was supported by R01HD114776 (RJC) and the Research Accelerator Program of the Shirley Ryan AbilityLab (RJC).

References

- [1] Richard S. Sutton and Andrew G. Barto. Reinforcement learning: An introduction. In *Reinforcement Learning: An Introduction*, chapter 17.6 Reinforcement Learning and the Future of Artificial Intelligence. MIT Press, Cambridge, MA, 2 edition, 2018. Chapter 17.6.
- [2] Christoph Dann, Yishay Mansour, and Mehryar Mohri. Reinforcement learning can be more efficient with multiple rewards. In Andreas Krause, Emma Brunskill, Kyunghyun Cho, Barbara Engelhardt, Sivan Sabato, and Jonathan Scarlett, editors, *Proceedings of the 40th International Conference on Machine Learning*, volume 202 of *Proceedings of Machine Learning Research*, pages 6948–6967. PMLR, 23–29 Jul 2023. URL <https://proceedings.mlr.press/v202/dann23a.html>.
- [3] Xue Bin Peng, Erwin Coumans, Tingnan Zhang, Tsang-Wei Lee, Jie Tan, and Sergey Levine. Learning Agile Robotic Locomotion Skills by Imitating Animals. In *Robotics: Science and Systems XVI*. Robotics: Science and Systems Foundation, July 2020. ISBN 978-0-9923747-6-1. doi: 10.15607/RSS.2020.XVI.064. URL <http://www.roboticsproceedings.org/rss16/p064.pdf>.
- [4] Coline Devin, Pieter Abbeel, Trevor Darrell, and Sergey Levine. Deep object-centric representations for generalizable robot learning. In *2018 IEEE International Conference on Robotics and Automation (ICRA)*, pages 7111–7118, 2018. doi: 10.1109/ICRA.2018.8461196.
- [5] Henry Zhu, Justin Yu, Abhishek Gupta, Dhruv Shah, Kristian Hartikainen, Avi Singh, Vikash Kumar, and Sergey Levine. The ingredients of real world robotic reinforcement learning. In *International Conference on Learning Representations*, 2020. URL <https://openreview.net/forum?id=rJe2syrtvS>.
- [6] Changyeon Kim, Jongjin Park, Jinwoo Shin, Honglak Lee, Pieter Abbeel, and Kimin Lee. Preference Transformer: Modeling Human Preferences using Transformers for RL, March 2023. URL <http://arxiv.org/abs/2303.00957>. arXiv:2303.00957 [cs].
- [7] Daniel M. Ziegler, Nisan Stiennon, Jeffrey Wu, Tom B. Brown, Alec Radford, Dario Amodei, Paul Christiano, and Geoffrey Irving. Fine-Tuning Language Models from Human Preferences, January 2020. URL <http://arxiv.org/abs/1909.08593>. arXiv:1909.08593 [cs].

- [8] OpenAI, Josh Achiam, Steven Adler, and et al. GPT-4 Technical Report, March 2024. URL <http://arxiv.org/abs/2303.08774>. arXiv:2303.08774 [cs].
- [9] Long Ouyang, Jeffrey Wu, Xu Jiang, and et al. Training language models to follow instructions with human feedback. In S. Koyejo, S. Mohamed, A. Agarwal, D. Belgrave, K. Cho, and A. Oh, editors, *Advances in Neural Information Processing Systems*, volume 35, pages 27730–27744. Curran Associates, Inc., 2022. URL https://proceedings.neurips.cc/paper_files/paper/2022/file/b1efde53be364a73914f58805a001731-Paper-Conference.pdf.
- [10] DeepSeek-AI, Daya Guo, Dejian Yang, and et al. DeepSeek-R1: Incentivizing Reasoning Capability in LLMs via Reinforcement Learning, January 2025. URL <http://arxiv.org/abs/2501.12948>. arXiv:2501.12948 [cs].
- [11] Dorsa Sadigh, Anca Dragan, Shankar Sastry, and Sanjit Seshia. Active Preference-Based Learning of Reward Functions. In *Robotics: Science and Systems XIII*. Robotics: Science and Systems Foundation, July 2017. ISBN 978-0-9923747-3-0. doi: 10.15607/RSS.2017.XIII.053. URL <http://www.roboticsproceedings.org/rss13/p53.pdf>.
- [12] Paul F Christiano, Jan Leike, Tom Brown, Miljan Martic, Shane Legg, and Dario Amodei. Deep Reinforcement Learning from Human Preferences. In I. Guyon, U. Von Luxburg, S. Bengio, H. Wallach, R. Fergus, S. Vishwanathan, and R. Garnett, editors, *Advances in Neural Information Processing Systems*, volume 30. Curran Associates, Inc., 2017. URL https://proceedings.neurips.cc/paper_files/paper/2017/file/d5e2c0adad503c91f91df240d0cd4e49-Paper.pdf.
- [13] Christian Wirth, Riad Akrou, Gerhard Neumann, and Johannes Fürnkranz. A Survey of Preference-Based Reinforcement Learning Methods. *Journal of Machine Learning Research*, 18(136):1–46, 2017. URL <http://jmlr.org/papers/v18/16-634.html>.
- [14] Ralph Allan Bradley and Milton E. Terry. Rank Analysis of Incomplete Block Designs: I. The Method of Paired Comparisons. *Biometrika*, 39(3/4):324–345, 1952. ISSN 0006-3444. doi: 10.2307/2334029. URL <https://www.jstor.org/stable/2334029>. Publisher: [Oxford University Press, Biometrika Trust].
- [15] Kimin Lee, Laura M. Smith, and Pieter Abbeel. PEBBLE: Feedback-Efficient Interactive Reinforcement Learning via Relabeling Experience and Unsupervised Pre-training. In *Proceedings of the 38th International Conference on Machine Learning*, pages 6152–6163. PMLR, July 2021. URL <https://proceedings.mlr.press/v139/lee21i.html>. ISSN: 2640-3498.
- [16] Donald Joseph Hejna III and Dorsa Sadigh. Few-shot preference learning for human-in-the-loop RL. In *6th Annual Conference on Robot Learning*, 2022. URL <https://openreview.net/forum?id=IKC5TfXLUW0>.
- [17] Joey Hejna, Rafael Rafailov, Harshit Sikchi, Chelsea Finn, Scott Niekum, W. Bradley Knox, and Dorsa Sadigh. Contrastive preference learning: Learning from human feedback without reinforcement learning. In *The Twelfth International Conference on Learning Representations*, 2024. URL <https://openreview.net/forum?id=iX1RjVQODj>.
- [18] Joey Hejna and Dorsa Sadigh. Inverse Preference Learning: Preference-based RL without a Reward Function. In A. Oh, T. Naumann, A. Globerson, K. Saenko, M. Hardt, and S. Levine, editors, *Advances in Neural Information Processing Systems*, volume 36, pages 18806–18827. Curran Associates, Inc., 2023. URL https://proceedings.neurips.cc/paper_files/paper/2023/file/3be7859b36d9440372cae0a293f2e4cc-Paper-Conference.pdf.
- [19] Gaon An, Junhyeok Lee, Xingdong Zuo, Norio Kosaka, Kyung-Min Kim, and Hyun Oh Song. Direct Preference-based Policy Optimization without Reward Modeling. In A. Oh, T. Naumann, A. Globerson, K. Saenko, M. Hardt, and S. Levine, editors, *Advances in Neural Information Processing Systems*, volume 36, pages 70247–70266. Curran Associates, Inc., 2023. URL https://proceedings.neurips.cc/paper_files/paper/2023/file/de8bd6b2b01cfa788e63f62e5b9a99b9-Paper-Conference.pdf.

- [20] Yachen Kang, Diyuan Shi, Jinxin Liu, Li He, and Donglin Wang. Beyond Reward: Offline Preference-guided Policy Optimization. In *Proceedings of the 40th International Conference on Machine Learning*, pages 15753–15768. PMLR, July 2023. URL <https://proceedings.mlr.press/v202/kang23b.html>. ISSN: 2640-3498.
- [21] Rafael Rafailov, Archit Sharma, Eric Mitchell, Christopher D Manning, Stefano Ermon, and Chelsea Finn. Direct Preference Optimization: Your Language Model is Secretly a Reward Model. In A. Oh, T. Naumann, A. Globerson, K. Saenko, M. Hardt, and S. Levine, editors, *Advances in Neural Information Processing Systems*, volume 36, pages 53728–53741. Curran Associates, Inc., 2023. URL https://proceedings.neurips.cc/paper_files/paper/2023/file/a85b405ed65c6477a4fe8302b5e06ce7-Paper-Conference.pdf.
- [22] Sachit Kuhar, Shuo Cheng, Shivang Chopra, Matthew Bronars, and Danfei Xu. Learning to Discern: Imitating Heterogeneous Human Demonstrations with Preference and Representation Learning. In *Proceedings of The 7th Conference on Robot Learning*, pages 1437–1449. PMLR, December 2023. URL <https://proceedings.mlr.press/v229/kuhar23a.html>. ISSN: 2640-3498.
- [23] Hao Sun, Yunyi Shen, and Jean-Francois Ton. Rethinking reward modeling in preference-based large language model alignment. In *The Thirteenth International Conference on Learning Representations*, 2025. URL <https://openreview.net/forum?id=rfdblE10qm>.
- [24] Yunhao Tang, Zhaohan Daniel Guo, Zeyu Zheng, Daniele Calandriello, Remi Munos, Mark Rowland, Pierre Harvey Richemond, Michal Valko, Bernardo Avila Pires, and Bilal Piot. Generalized preference optimization: A unified approach to offline alignment. In Ruslan Salakhutdinov, Zico Kolter, Katherine Heller, Adrian Weller, Nuria Oliver, Jonathan Scarlett, and Felix Berkenkamp, editors, *Proceedings of the 41st International Conference on Machine Learning*, volume 235 of *Proceedings of Machine Learning Research*, pages 47725–47742. PMLR, 21–27 Jul 2024. URL <https://proceedings.mlr.press/v235/tang24b.html>.
- [25] Remi Munos, Michal Valko, Daniele Calandriello, Mohammad Gheshlaghi Azar, Mark Rowland, Zhaohan Daniel Guo, Yunhao Tang, Matthieu Geist, Thomas Mesnard, Côme Fiegel, Andrea Michi, Marco Selvi, Sertan Girgin, Nikola Momchev, Olivier Bachem, Daniel J Mankowitz, Doina Precup, and Bilal Piot. Nash learning from human feedback. In Ruslan Salakhutdinov, Zico Kolter, Katherine Heller, Adrian Weller, Nuria Oliver, Jonathan Scarlett, and Felix Berkenkamp, editors, *Proceedings of the 41st International Conference on Machine Learning*, volume 235 of *Proceedings of Machine Learning Research*, pages 36743–36768. PMLR, 21–27 Jul 2024. URL <https://proceedings.mlr.press/v235/munos24a.html>.
- [26] Mohammad Azar, Zhaohan Daniel Guo, Bilal Piot, Remi Munos, Mark Rowland, Michal Valko, and Daniele Calandriello. A general theoretical paradigm to understand learning from human preferences. In Sanjoy Dasgupta, Stephan Mandt, and Yingzhen Li, editors, *Proceedings of The 27th International Conference on Artificial Intelligence and Statistics*, volume 238 of *Proceedings of Machine Learning Research*, pages 4447–4455. PMLR, 02–04 May 2024. URL <https://proceedings.mlr.press/v238/gheshlaghi-azar24a.html>.
- [27] Chenlu Ye, Wei Xiong, Yuheng Zhang, Hanze Dong, Nan Jiang, and Tong Zhang. Online Iterative Reinforcement Learning from Human Feedback with General Preference Model. In A. Globerson, L. Mackey, D. Belgrave, A. Fan, U. Paquet, J. Tomczak, and C. Zhang, editors, *Advances in Neural Information Processing Systems*, volume 37, pages 81773–81807. Curran Associates, Inc., 2024. URL https://proceedings.neurips.cc/paper_files/paper/2024/file/94d13c2401fe119e57ba325b6fe526e0-Paper-Conference.pdf.
- [28] Amos Tversky. Intransitivity of preferences. *Psychological Review*, 76(1):31–48, January 1969. ISSN 1939-1471, 0033-295X. doi: 10.1037/h0026750. URL <https://doi.apa.org/doi/10.1037/h0026750>.
- [29] Kenneth O. May. Intransitivity, Utility, and the Aggregation of Preference Patterns. *Econometrica*, 22(1):1–13, 1954. URL <https://onlinelibrary.wiley.com/doi/abs/10.1086/22811>; 1: IUATA0 > 2.0.CO; 2-P.

- [30] Jie Cheng, Gang Xiong, Xingyuan Dai, Qinghai Miao, Yisheng Lv, and Fei-Yue Wang. RIME: robust preference-based reinforcement learning with noisy preferences. In *Proceedings of the 41st International Conference on Machine Learning*, volume 235 of *ICML'24*, pages 8229–8247, Vienna, Austria, July 2024. JMLR.org.
- [31] Yann Dubois, Chen Xuechen Li, Rohan Taori, Tianyi Zhang, Ishaan Gulrajani, Jimmy Ba, Carlos Guestrin, Percy S Liang, and Tatsunori B Hashimoto. AlpacaFarm: A Simulation Framework for Methods that Learn from Human Feedback. In A. Oh, T. Naumann, A. Globerson, K. Saenko, M. Hardt, and S. Levine, editors, *Advances in Neural Information Processing Systems*, volume 36, pages 30039–30069. Curran Associates, Inc., 2023. URL https://proceedings.neurips.cc/paper_files/paper/2023/file/5fc47800ee5b30b8777fdd30abcaaf3b-Paper-Conference.pdf.
- [32] Thomas Coste, Usman Anwar, Robert Kirk, and David Krueger. Reward model ensembles help mitigate overoptimization. In *The Twelfth International Conference on Learning Representations*, 2024. URL <https://openreview.net/forum?id=dcjtMYkpXx>.
- [33] Kimin Lee, Laura Smith, Anca Dragan, and Pieter Abbeel. B-pref: Benchmarking preference-based reinforcement learning. In *Thirty-fifth Conference on Neural Information Processing Systems Datasets and Benchmarks Track (Round 1)*, 2021. URL https://openreview.net/forum?id=ps95-mkHF_.
- [34] Yi Ma, Jianye Hao, Hebin Liang, and Chenjun Xiao. Rethinking decision transformer via hierarchical reinforcement learning. In *Proceedings of the 41st International Conference on Machine Learning*, volume 235 of *ICML'24*, pages 33730–33745, Vienna, Austria, July 2024. JMLR.org.
- [35] Prajjwal Bhargava, Rohan Chitnis, Alborz Geramifard, Shagun Sodhani, and Amy Zhang. WHEN SHOULD WE PREFER DECISION TRANSFORMERS FOR OFFLINE REINFORCEMENT LEARNING? 2024.
- [36] Ilya Kostrikov, Ashvin Nair, and Sergey Levine. OFFLINE REINFORCEMENT LEARNING WITH IMPLICIT Q-LEARNING. 2022.
- [37] Minu Kim, Yongsik Lee, Sehyeok Kang, Jihwan Oh, Song Chong, and Se-Young Yun. Preference Alignment with Flow Matching. In A. Globerson, L. Mackey, D. Belgrave, A. Fan, U. Paquet, J. Tomczak, and C. Zhang, editors, *Advances in Neural Information Processing Systems*, volume 37, pages 35140–35164. Curran Associates, Inc., 2024. URL https://proceedings.neurips.cc/paper_files/paper/2024/file/3df874367ce2c43891aab1ab23ae6959-Paper-Conference.pdf.
- [38] Zhilong Zhang, Yihao Sun, Junyin Ye, Tian-Shuo Liu, Jiaji Zhang, and Yang Yu. Flow to better: Offline preference-based reinforcement learning via preferred trajectory generation. In *The Twelfth International Conference on Learning Representations*, 2024. URL <https://openreview.net/forum?id=EG68RSznLT>.
- [39] Wenjie Wang, Fuli Feng, Xiangnan He, Liqiang Nie, and Tat-Seng Chua. Denoising Implicit Feedback for Recommendation. In *Proceedings of the 14th ACM International Conference on Web Search and Data Mining*, pages 373–381, Virtual Event Israel, March 2021. ACM. ISBN 978-1-4503-8297-7. doi: 10.1145/3437963.3441800. URL <https://dl.acm.org/doi/10.1145/3437963.3441800>.
- [40] Hongyi Zhang, Moustapha Cisse, Yann N Dauphin, and David Lopez-Paz. mixup: BEYOND EMPIRICAL RISK MINIMIZATION. 2018.
- [41] Bo Han, Quanming Yao, Xingrui Yu, Gang Niu, Miao Xu, Weihua Hu, Ivor Tsang, and Masashi Sugiyama. Co-teaching: Robust training of deep neural networks with extremely noisy labels. In S. Bengio, H. Wallach, H. Larochelle, K. Grauman, N. Cesa-Bianchi, and R. Garnett, editors, *Advances in Neural Information Processing Systems*, volume 31. Curran Associates, Inc., 2018. URL https://proceedings.neurips.cc/paper_files/paper/2018/file/a19744e268754fb0148b017647355b7b-Paper.pdf.

- [42] Michal Lukasik, Srinadh Bhojanapalli, Aditya Krishna Menon, and Sanjiv Kumar. Does label smoothing mitigate label noise? In *Proceedings of the 37th International Conference on Machine Learning*, volume 119 of *ICML'20*, pages 6448–6458. JMLR.org, July 2020.
- [43] Hwanjun Song, Minseok Kim, Dongmin Park, Yooju Shin, and Jae-Gil Lee. Learning from noisy labels with deep neural networks: A survey. *IEEE Transactions on Neural Networks and Learning Systems*, 34(11):8135–8153, 2023. doi: 10.1109/TNNLS.2022.3152527.
- [44] Ashish Vaswani, Noam Shazeer, Niki Parmar, Jakob Uszkoreit, Llion Jones, Aidan N Gomez, Łukasz Kaiser, and Illia Polosukhin. Attention is All you Need. In I. Guyon, U. Von Luxburg, S. Bengio, H. Wallach, R. Fergus, S. Vishwanathan, and R. Garnett, editors, *Advances in Neural Information Processing Systems*, volume 30. Curran Associates, Inc., 2017. URL https://proceedings.neurips.cc/paper_files/paper/2017/file/3f5ee243547dee91fbd053c1c4a845aa-Paper.pdf.
- [45] Ting Chen, Simon Kornblith, Mohammad Norouzi, and Geoffrey Hinton. A Simple Framework for Contrastive Learning of Visual Representations. In *Proceedings of the 37th International Conference on Machine Learning*, pages 1597–1607. PMLR, November 2020. URL <https://proceedings.mlr.press/v119/chen20j.html>. ISSN: 2640-3498.
- [46] Justin Fu, Aviral Kumar, Ofir Nachum, George Tucker, and Sergey Levine. D4RL: Datasets for Deep Data-Driven Reinforcement Learning, February 2021. URL <http://arxiv.org/abs/2004.07219>. arXiv:2004.07219 [cs].
- [47] Ritwik Gupta. D4RL: Building Better Benchmarks for Offline Reinforcement Learning. URL <http://bair.berkeley.edu/blog/2020/06/25/D4RL/>.
- [48] MuJoCo - Gym Documentation. URL <https://www.gymnasium.dev/environments/mujoco/index.html>.
- [49] Yihao Sun. Offlinerl-kit: An elegant pytorch offline reinforcement learning library. <https://github.com/yihaosun1124/OfflineRL-Kit>, 2023.
- [50] Donald Hejna, Lerrel Pinto, and Pieter Abbeel. Hierarchically decoupled imitation for morphological transfer. In Hal Daumé III and Aarti Singh, editors, *Proceedings of the 37th International Conference on Machine Learning*, volume 119 of *Proceedings of Machine Learning Research*, pages 4159–4171. PMLR, 13–18 Jul 2020. URL <https://proceedings.mlr.press/v119/hejna20a.html>.
- [51] Runze Liu, Yali Du, Fengshuo Bai, Jiafei Lyu, and Xiu Li. PEARL: Zero-shot cross-task preference alignment and robust reward learning for robotic manipulation. In Ruslan Salakhutdinov, Zico Kolter, Katherine Heller, Adrian Weller, Nuria Oliver, Jonathan Scarlett, and Felix Berkenkamp, editors, *Proceedings of the 41st International Conference on Machine Learning*, volume 235 of *Proceedings of Machine Learning Research*, pages 30946–30964. PMLR, 21–27 Jul 2024. URL <https://proceedings.mlr.press/v235/liu24o.html>.
- [52] Alejandro Escontrela, Xue Bin Peng, Wenhao Yu, Tingnan Zhang, Atıl İscen, Ken Goldberg, and Pieter Abbeel. Adversarial Motion Priors Make Good Substitutes for Complex Reward Functions. In *2022 IEEE/RSJ International Conference on Intelligent Robots and Systems (IROS)*, pages 25–32, October 2022. doi: 10.1109/IROS47612.2022.9981973. URL <https://ieeexplore.ieee.org/document/9981973/>. ISSN: 2153-0866.
- [53] Takahiro Miki, Joonho Lee, Jemin Hwangbo, Lorenz Wellhausen, Vladlen Koltun, and Marco Hutter. Learning robust perceptive locomotion for quadrupedal robots in the wild. *Science Robotics*, 7(62):eabk2822, January 2022. doi: 10.1126/scirobotics.abk2822. URL <https://www.science.org/doi/10.1126/scirobotics.abk2822>. Publisher: American Association for the Advancement of Science.
- [54] Saran Tunyasuvunakool, Alistair Muldal, Yotam Doron, Siqi Liu, Steven Bohez, Josh Merel, Tom Erez, Timothy Lillicrap, Nicolas Heess, and Yuval Tassa. dm_control: Software and tasks for continuous control. *Software Impacts*, 6:100022, 2020. ISSN 2665-9638. doi: <https://doi.org/10.1016/j.simpa.2020.100022>. URL <https://www.sciencedirect.com/science/article/pii/S2665963820300099>.

- [55] Michael Laskin, Denis Yarats, Hao Liu, Kimin Lee, Albert Zhan, Kevin Lu, Catherine Cang, Lerrel Pinto, and Pieter Abbeel. URLB: Unsupervised reinforcement learning benchmark. In *Thirty-fifth Conference on Neural Information Processing Systems Datasets and Benchmarks Track (Round 2)*, 2021. URL https://openreview.net/forum?id=lwrPkQP_is.
- [56] Timothy P. Lillicrap, Jonathan J. Hunt, Alexander Pritzel, Nicolas Heess, Tom Erez, Yuval Tassa, David Silver, and Daan Wierstra. Continuous control with deep reinforcement learning. In Yoshua Bengio and Yann LeCun, editors, *ICLR*, 2016. URL <https://arxiv.org/abs/1509.02971>.
- [57] TransformerEncoder — PyTorch 2.7 documentation. URL <https://docs.pytorch.org/docs/stable/generated/torch.nn.TransformerEncoder.html>.
- [58] Hopper - Gym Documentation. URL <https://www.gymnasium.dev/environments/mujoco/hopper/>.
- [59] Walker2D - Gym Documentation. URL <https://www.gymnasium.dev/environments/mujoco/walker2d/>.

A Motivation for SARA reward inference

A full theoretical treatment is suggested for future works, but here we provide motivation for our proposed reward estimation detailed in Section 3. Sun et al. [23] examined preference learning in a LLM context, and they noted that BT formulations are not necessary. Instead of a BT loss that predicts the probability of preferring one response over another, they proposed a simple classifier approach of predicting preference (1 or 0 labeling) for the responses. They showed that such an approach preserves the ordering of the underlying true reward function, and that it is sufficient for downstream LLM alignment. Thus, instead of predicting the BT $P[\sigma^1 \succ \sigma^0; \psi]$ for a reward model parameterized by ψ , it is sufficient to predict $P[\sigma^i; \psi]$ with $i \in \{0, 1\}$ [23]. In the next paragraph, we show that our approach implicitly does the same.

While our work focuses on representation learning followed by reward inference, their model focuses on classification for learning an explicit reward model. Nonetheless, their work provides theoretical grounding for our proposal that we learn based on individual trajectory labelings of preferred vs. non-preferred rather than learning the BT-based relative rankings. As discussed in Section 3, we train a contrastive encoder to separate preferred from non-preferred latents using the cosine-similarity based SimCLR loss [45]. Subsequently, we pass our full set of preferred trajectories and full set of non-preferred trajectories through the encoder to get our representations, \mathbf{z}_p^* and \mathbf{z}_n^* , respectively. Now consider a sampled trajectory σ_t for which we would like to compute the reward. We can pass σ_t through our trained SARA encoder to get \mathbf{z}_t . We then propose the following proxy estimate for the probability of the sampled trajectory σ_t being preferred, given its latent representation:

$$P(p | \mathbf{z}_t) = \frac{\exp(\cos(\mathbf{z}_t, \mathbf{z}_p^*))}{\exp(\cos(\mathbf{z}_t, \mathbf{z}_p^*)) + \exp(\cos(\mathbf{z}_t, \mathbf{z}_n^*))} \tag{1}$$

$$= \frac{1}{1 + \exp(-[\cos(\mathbf{z}_t, \mathbf{z}_p^*) - \cos(\mathbf{z}_t, \mathbf{z}_n^*)])}. \tag{2}$$

Such a probability function is a natural choice because the SimCLR loss aligns and separates latents using exponentiated cosine similarities. In RL we want to incentivize actions that have high probability of being preferred. Therefore, we simply set our reward equal to $r_t = \cos(\mathbf{z}_t, \mathbf{z}_p^*) - \alpha \cos(\mathbf{z}_t, \mathbf{z}_n^*)$, where $\alpha \geq 0$ is a hyperparameter to control the trade-off between the two terms. Empirically, we found $\alpha = 0$ to be optimal in all our experiments (both the offline and the online reward shaping experiments). With that, we recover our proposed reward in Section 3. Similar to Sun et al. [23], we score trajectories on their alignment with preferred trajectories rather than relying on potentially noisy relative labels.

B Additional offline RL results

B.1 Locomotion and kitchen tasks

The main paper provides the tables for human-labeled preference sets with neutral queries (the original unmodified data) and the human-labeled preference sets with 20% error. Here we provide the tables for human-labeled preference sets without neutral queries and script labeled preference sets.

Table 3: Average normalized policy evaluation rewards (across 8 seeds), using **human-labeled preference data without neutral preferences**. Values in **bold** are best (highest reward) in each row and underlined are within 1% of best. The \pm denotes standard deviation.

Task	IQL (Oracle)	PT	PT+ADT	DPPO	SARA
hopper-replay	92.26 \pm 13.6	86.67 \pm 4.7	83.06 \pm 8.8	70.18 \pm 19.9	84.43 \pm 4.3
hopper-expert	80.82 \pm 44.5	59.90 \pm 46.2	74.53 \pm 41.7	108.88 \pm 9.5	80.93 \pm 43.9
walker2d-replay	77.53 \pm 15.5	75.14 \pm 3.9	76.69 \pm 6.5	47.87 \pm 27.6	78.21 \pm 5.8
walker2d-expert	107.57 \pm 8.5	110.09 \pm 4.6	<u>109.61</u> \pm 2.2	108.77 \pm 0.4	108.91 \pm 3.4
kitchen-partial	44.88 \pm 31.4	61.64 \pm 15.0	<u>60.78</u> \pm 15.1	39.77 \pm 18.9	63.79 \pm 14.6
kitchen-mixed	54.02 \pm 16.4	50.66 \pm 13.8	52.11 \pm 12.5	45.35 \pm 17.9	<u>51.80</u> \pm 7.2

Table 4: Average normalized policy evaluation rewards (across 8 seeds), using **script-labeled preference data**. Values in **bold** are best (highest reward) in each row and underlined are within 1% of best. The \pm denotes standard deviation.

Task	IQL (Oracle)	PT	PT+ADT	DPPO	SARA
hopper-replay	92.26 \pm 13.6	38.43 \pm 19.8	70.55 \pm 33.8	32.75 \pm 22.6	87.43 \pm 8.4
hopper-expert	80.82 \pm 44.5	63.03 \pm 34.5	86.96 \pm 35.9	102.19 \pm 24.4	96.43 \pm 27.9
walker2d-replay	77.53 \pm 15.5	76.69 \pm 14.0	<u>76.40</u> \pm 11.0	52.27 \pm 24.7	<u>76.51</u> \pm 6.4
walker2d-expert	107.57 \pm 8.5	109.80 \pm 1.9	<u>109.74</u> \pm 1.0	<u>108.81</u> \pm 0.4	<u>108.88</u> \pm 4.6
kitchen-partial	44.88 \pm 31.4	68.32 \pm 12.2	<u>62.58</u> \pm 20.6	38.28 \pm 18.6	56.05 \pm 20.9
kitchen-mixed	54.02 \pm 16.4	47.58 \pm 18.2	49.10 \pm 14.3	44.77 \pm 17.8	49.84 \pm 11.2

B.2 Offline RL results on Adroit tasks

We also applied our framework to the Adroit tasks, with preference datasets for pen-cloned-v1 and pen-human-v1 provided by Kim et al. [6]. DPPO underperforms compared to other methods on pen-human-v1, but otherwise the mean evaluation policy rewards are similar across models (Tables 5, 6, 7, and 8). Variance is also quite high for all models. This is explained by within seed variance among the 10 evaluation episodes at each epoch, presumably due to randomized initial start states, as opposed to across seed variance. Among the 10 evaluation episodes at each epoch, we acquire maximum normalized episode returns of 179 and minimum returns between -2 to -4.

Table 5: Average normalized policy evaluation rewards (across 8 seeds), using **human-labeled preference data with 20% label error rate**. Values in **bold** are best (highest reward) in each row. The \pm denotes standard deviation.

Task	IQL (Oracle)	PT	PT+ADT	DPPO	SARA
pen-human-v1	85.19 (\pm 62.1)	81.91 (\pm 64.5)	79.42 (\pm 63.2)	71.99 (\pm 62.5)	83.04 (\pm 63.6)
pen-cloned-v1	81.49 (\pm 62.6)	69.30 (\pm 63.8)	67.66 (\pm 64.1)	72.64 (\pm 64.4)	69.78 (\pm 63.0)

C Dataset details

Here we describe the details of the preference datasets and the full offline datasets used for our offline RL experiments (Section 4)

Table 6: Average normalized policy evaluation rewards (across 8 seeds), using **human-labeled preference data with neutral preferences**. Values in **bold** are best (highest reward) in each row. The \pm denotes standard deviation.

Task	IQL (Oracle)	PT	PT+ADT	DPPO	SARA
pen-human-v1	85.19 (± 62.1)	80.84 (± 63.1)	82.80 (± 62.4)	76.97 (± 64.3)	81.89 (± 63.2)
pen-cloned-v1	81.49 (± 62.6)	70.28 (± 64.6)	69.70 (± 63.8)	72.13 (± 64.5)	69.72 (± 63.4)

Table 7: Average normalized policy evaluation rewards (across 8 seeds), using **human-labeled preference data without neutral preferences**. Values in **bold** are best (highest reward) in each row and underlined are within 1% of best. The \pm denotes standard deviation.

Task	IQL (Oracle)	PT	PT+ADT	DPPO	SARA
pen-human-v1	85.19 (± 62.1)	83.59 (± 62.8)	85.06 (± 61.7)	75.51 (± 63.8)	81.52 (± 62.4)
pen-cloned-v1	81.49 (± 62.6)	70.18 (± 64.0)	69.70 (± 64.3)	<u>70.95</u> (± 65.6)	71.07 (± 64.3)

Table 8: Average normalized policy evaluation rewards (across 8 seeds), using **script-labeled preference data**. Values in **bold** are best (highest reward) in each row and underlined are within 1% of best. The \pm denotes standard deviation.

Task	IQL (Oracle)	PT	PT+ADT	DPPO	SARA
pen-human-v1	85.19 (± 62.1)	81.67 (± 62.8)	<u>82.80</u> (± 63.8)	71.62 (± 66.0)	83.06 (± 63.0)
pen-cloned-v1	81.49 (± 62.6)	76.88 (± 65.3)	74.30 (± 65.3)	75.41 (± 64.6)	73.38 (± 65.6)

C.1 Preference datasets

For Mujoco locomotion and Adroit pen tasks, we use the preference datasets provided by Kim et al. [6] from the PT human label repository. For the Franka Kitchen tasks, we use the preference datasets from An et al. [19] from the DPPO human label repository. Both repositories are MIT licensed.

Kim et al. [6] and An et al. [19] created the preference datasets by sampling pairs of trajectories from the full offline datasets [46]. They named the preference datasets by the same name as the full offline datasets (e.g. hopper-medium-replay-v2 and so on). All trajectories are 100 timesteps in length. The replay datasets for hopper and walker have 500 trajectory pairs and all others have 100 pairs. The labelers are domain experts who are given specific criteria upon which to evaluate their preference for the trajectories. We refer the reader to the original works which state their preference criteria. Excluding pairs with equally preferred trajectories is one of our dataset variants, so here we provide the number of such queries in each dataset (Table 9).

C.2 Full offline datasets

In our offline RL experiments, the policies for the SARA framework, all baselines, and the oracle are trained using the full offline D4RL datasets. The oracle uses the true environmental rewards provided in the datasets. In the case of the SARA framework and baseline models, each transition reward is computed using the respective models. Note all these models are non-Markovian, so each transition reward at time t is computed by feeding the trajectory up to and including time t into the models. For each model, we replace the dataset provided rewards with the computed transition rewards.

We refer to the work by Fu et al. [46] for a thorough description of the full offline datasets. Here we summarize some key points as they relate to our work. Our experiments include hopper and walker2d locomotion tasks from Gym-Mujoco. The hopper has a 3 dimensional action space and 11 dimensional state space. The walker2d has a 6 dimensional action space and 17 dimensional state space. Franka Kitchen tasks are multi-task and high dimensional, requiring algorithms to "stitch" trajectories. The action space is 9 dimensional and the state space is 60 dimensional. The Adroit pen tasks are also high dimensional and contain a narrow distribution of expert or cloned expert data. The action space is 24-dimensional and the state space is 55-dimensional. By testing the methods on the 8 datasets from these three environments, we experiment on a range of task dimensionalities and difficulties.

Table 9: Percentage of neutral queries by preference set.

Preference Set	Total Pairs	Neutral (%)
hopper-medium-replay-v2	500	38%
hopper-medium-expert-v2	100	28%
walker2d-medium-replay-v2	500	23%
walker2d-medium-expert-v2	100	24%
kitchen-partial-v0	100	22%
kitchen-mixed-v0	100	24%
pen-human-v1	100	35%
pen-cloned-v1	100	40%

D SARA framework architecture and hyperparameters

First we provide the architecture of our contrastive encoder. Then we provide the hyperparameters used for acquiring the results in our main paper.

D.1 Transformer architecture

Here we briefly summarize architecture and hyperparameters for our contrastive encoder. Both Transformer Encoders use the standard Pytorch implementation [57], which is based upon the originally proposed Transformer architecture by Vaswani et al. [44]. The Transformer Encoder 1 encodes each trajectory (state and action sequences), but it does not enable attention between trajectories. Information at different timesteps within each trajectory can attend to one another. We inject temporal information via positional encoding [44]. We experimented with causal masking in the encoder training, where state-actions can only attend to previous state-actions but not future. However, we found that this masking made either no difference or slightly degraded performance in downstream IQL learning.

We conduct average pooling over timesteps for each trajectory, resulting in one latent per trajectory: $\mathbf{u}_{p/n,i}$, where p or n indicates preferred or non-preferred and i indexes trajectory. Next we form k subsets within each category, *i.e.* k subsets within the set of $\{\mathbf{u}_{p,i}\}$ and k subsets within the set of $\{\mathbf{u}_{n,i}\}$. Each subset is comprised solely of trajectories for either preferred or non-preferred. Then we pass each subset $\{\mathbf{u}_p\}_k$ and $\{\mathbf{u}_n\}_k$ through Transformer Encoder 2, enabling encodings in the same subset to attend to each other. Note the time dimension was already removed prior to this encoder, so we do not have any positional encoding here. We then have single encoding $\mathbf{z}_{p/n,k}$ for each subset. This is trained with the SimCLR loss with a temperature hyperparameter [45]. The SimCLR loss does the following: pulls together latents within the same type (p or n) and repels each of the $\{\mathbf{z}_{p,k}\}$ from each of the $\{\mathbf{z}_{n,k}\}$. As noted in Section 3, we shuffle the composition of latents in each subset $\{\mathbf{u}_p\}_k$ and $\{\mathbf{u}_n\}_k$ to ensure robustness to mislabeling or existence of similar trajectories in the two sets.

As noted in the main paper, we conduct each experiments over 8 seeds. The seeding not only applies to the downstream IQL training but also the encoder training. We do this to align with our baseline models [6, 19], which also seed their Preference Transformer and DPPO Probability Predictor, respectively, with the same seed as their downstream policy training.

D.2 SARA encoder hyperparameters

Unless otherwise noted, all hyperparameters were kept the same for all preference datasets, even though the Kitchen and Adroit environments have higher dimensional action/state spaces than the locomotion tasks.

Here we provide hyperparameters for both Transformer Encoder 1 and Transformer Encoder 2

Here we provide additional training hyperparameters:

The sequence lengths in the preference sets are all 100. As done by the DDPO baseline [19], we experimented with using subsequences of varying lengths in training. We passed in subsequence lengths of [10, 20, 30, 40, 50, 60, 70, 80, 90, 100], and we used random start points in the sequences.

Table 10: Transformer Encoder 1 and 2 Hyperparameters

Hyperparameter	Value
Causal pooling	No
Model dimension (d_{model})	256
Feedforward network dimension	256
Embedding dimension ($\mathbf{z}_{p/n}$ dim)	16
Encoder dropout rate	0.0
Positional encoding dropout rate	0.0
Number of encoder layers	1
Number of attention heads	4
Avg pooling (after 1st encoder)	Yes

Table 11: Training Hyperparameters

Hyperparameter	Value
Batch size	256
Use cosine learning-rate schedule	Yes
Initial learning rate	1×10^{-5}
Min learning rate	1×10^{-6}
Optimizer	Adam
Number of epochs	2000 (hopper expert), 10^4 (walker replay), 4000 (all others)
Sets per category (k)	2
Temperature (SimCLR loss)	0.1

We found that using random subsequences to train the encoder resulted in slightly reduced variance in the downstream IQL training on the hopper replay dataset. However, in general the asymptotic performance in IQL training was not sensitive to whether or not we used random subsequences of varying length.

E Policy training and evaluation

We first provide details regarding policy training. We then detail the evaluation method.

E.1 Policy training hyperparameters

We train policies for oracle, SARA, PT, and PT+ADT using the IQL implementation in the publicly available OfflineRL-kit [49]. We carefully match hyperparameters to those suggested by Kim et al. [6], which also match the hyperparameters suggested for the offline datasets in Kostrikov et al. [36]. In these works, the Gym-Mujoco environments have different IQL hyperparameters, namely for dropout and temperature, than the ones used for the Franka Kitchen and Adroit environments. We also use the same reward normalization functions provided by Kim et al. [6]. We also carefully match hyperparameters for DPPO policy training to the ones provided by An et al. [19] in their appendices and code repository. We defer to Kim et al. [6] and An et al. [19] for exact hyperparameters. Upon acceptance, we will release our IQL training pipeline with the hyperparameters used for each offline dataset.

E.2 Policy evaluation method

To compare methods, we roll out multiple evaluation episodes for the method’s learned policy and get the normalized trajectory reward provided by the environment, as done in prior PbRL works. We use the *get_normalized_score* functions provided by each environment, which uses scaling factors unique to that environment. We scale the episode returns by 100 as done in prior works.

To avoid reporting overly optimistic values, we follow the method proposed by Hejna et al. [17]. We roll out 10 evaluation episodes every 5 epochs of training. We compute the average and the standard deviation of the true normalized episode rewards over the last 8 evaluations. Thus 80 total evaluation

episode rewards are averaged at each epoch. This running mean is averaged over the 8 seeds. We report the maximum value achieved after averaging the running mean over the seeds. As noted in [17], this maximum of seed-averaged running mean mitigates effects of stochasticity. Past works either do not provide details on the metric computation or report the seed-averaged maximum, which can inflate performance. To report standard deviations that capture both within-seed and across-seed variability, we compute the total standard deviation as follows.

At each epoch of training a particular seed $s \in \{1, \dots, S\}$, we have a set of $n = 80$ evaluation episodes. For each seed, we compute the standard deviation over episodes and apply Bessel’s correction:

$$\sigma_s^{\text{corrected}} = \sigma_s \cdot \sqrt{\frac{n}{n-1}}.$$

The *within-seed variance* is the average of squared corrected standard deviations:

$$\sigma_{\text{within}}^2 = \frac{1}{S} \sum_{s=1}^S (\sigma_s^{\text{corrected}})^2.$$

Let μ_s denote the mean return for seed s . The *across-seed variance* is the unbiased sample variance of the seed means:

$$\sigma_{\text{across}}^2 = \frac{1}{S-1} \sum_{s=1}^S (\mu_s - \bar{\mu})^2, \quad \bar{\mu} = \frac{1}{S} \sum_{s=1}^S \mu_s.$$

The total standard deviation used for error bars is then given by:

$$\sigma_{\text{total}} = \sqrt{\sigma_{\text{within}}^2 + \sigma_{\text{across}}^2}.$$

We use the same seeds and reporting methods for all reported values, including for SARA, baselines, and the oracle.

F Cross-task transfer of preferences

Table 12: Hopper to walker2d action and observation dim mapping

Action Mapping		
hopper dims	walker2d dims	actions in walker2d
0–2	0–2	torques on thigh, leg, foot joints (right)
0–2	3–5	torques on thigh, leg, foot joints (left)
Observations Mapping		
hopper dims	walker2d dims	observations in walker2d
0–1	0–1	height and angle of top of torso
2–4	2–4	angle of thigh, leg, foot joints (right)
2–4	5–7	angle of thigh, leg, foot joints (left)
5–7	8–10	velocity of x coordinate, height coordinate, and angular velocity of top
8–10	11–13	angular velocities of thigh, leg, foot hinges (right)
8–10	14–16	angular velocities of thigh, leg, foot hinges (left)

As discussed in Section 5 we train on the hopper-medium-replay-v2 preference set, and we use the learned preferred latent to compute rewards for the full offline walker2d-medium-replay-v2 dataset. We then conduct IQL training on this walker2d dataset. In order to accomplish the SARA reward computation we must build an encoder based on the hopper data that can accept walker state-action space dimensions. The online Gym documentation provides a detailed description of the hopper and walker2d state and action spaces [58, 59]. We need to map the 3-dimensional hopper action space to the 6-dimensional walker2d action space. We also need to map the 11-dimensional hopper state

space to the 17-dimensional walker2d state space. To do so we exploit the symmetries in the walker joints as shown in Table 12.

Of course this is not a physically realistic way to map the dimensions. In a well trained walker2d policy, the two legs are not moving symmetrically. Nonetheless, we train an encoder on the hopper replay data with dimensions mapped in this way, and subsequently we infer a preferred latent with this modified hopper replay data. Next, we take the full offline D4RL walker2d replay dataset, and we pass each trajectory through the encoder to get latents for each timestep in each trajectory. Next we compute rewards for each timestep in each trajectory in the walker2d replay dataset by computing cosine similarity with the preferred latent. Lastly we conduct IQL training and evaluate as we did with all other datasets. Though we based this method on physically unrealistic assumptions, we acquire normalized policy rewards that are only few points worse than the reward values attained using the walker2d replay preference set (Figure 4). We also result in lower evaluation reward variance compared to the oracle.

G Compute resources

Our experiments involved training the following individual models on multiple seeds and datasets: SARA contrastive encoder, PT, PT+ADT, IQL policy training, DPPO preference predictor, and DPPO policy. Each individual model was trained on a single NVIDIA A100-SXM4-80GB GPU and 16 CPU cores. Compute resources needed were less than 20GB GPU per model. Training time for the SARA encoder, PT, PT+ADT, and DPPO preference predictor varies depending on size of dataset and number of epochs, but it was typically under 30 minutes per model. The walker2d-medium-replay-v2 dataset took up to 2 hours to train a SARA encoder for 10000 epochs when using additional random slices of trajectories. The DPPO policy training took approximately 2 hours to train on one model on the single GPU. The IQL policy training, using the open source OfflineRL-kit [49], took about 3.5 hours to train one model. These computing resources were used for 8 datasets, each model, and 8 seeds per model+dataset. We used our university’s computing cluster with access to multiple GPUs, but the models could also be trained on a single standalone GPU or with increased training time, on CPUs alone.